8th High Performance Yacht Design Conference (HPYD 8)
21st – 22nd March, 2024
Auckland, New Zealand
www.HPYD.org.nz

HPYD 8
2024
AUCKLAND NZ

Aerodynamic Performance of a 68m Ketch Sailing Yacht Obtained from Wind Tunnel Tests

Etienne Gauvain
Wolfson Unit MTIA, UK.

Mark Leslie-Miller
Dykstra Naval Architects, The Netherlands.

Abstract. Multi-masted rigs frequently found on large superyachts offer a number of complex challenges for sail designers and naval architects. They create complex aerodynamic interactions with their cascade of sails and large number of sheeting options. Evaluating the aerodynamic performance of a sailplan can help towards the design of a well-balanced and performant yacht.

This paper presents wind tunnel tests carried out on a scale model of the 68m ketch *Project Zero*. The tests were conducted with the aim of evaluating the performance of sailplan options across a range of upwind, offwind and reefed configurations and the effects of sail settings upon longitudinal centre of effort location with various sail combinations.

The principal aim of the paper is to share with the yacht engineering community the aerodynamic performance of *Project Zero* obtained from wind tunnel tests, thanks to the dedication of *Foundation Zero*. This data can be used by yacht designers and researchers to help validate and even refine their numerical tools and to offer a starting point values in the absence of other data sources.

Keywords: aerodynamics; performance; multi-masted rigs; sailing yachts; wind tunnel.

NOMENCLATURE

α	Angle of Attack	F_{HEEL}	Heeling Force
β	Apparent Wind Angle	F_{SIDE}	Side Force
ε_A	Aerodynamic Force Angle	F_{VERT}	Vertical Force
φ	Heel Angle	M_{PITCH}	Pitch Moment
ρ	Air Density	M_{ROLL}	Roll Moment
		M_{YAW}	Yaw Moment
AEX	Aero Experimental Sailset File	q	Dynamic Pressure
AWA	Apparent Wind Angle	RM	Righting Moment
AWS	Apparent Wind Speed	Ref Area	Ref. Sail Area of Configuration
Ax, Ay	Frontal, Lateral Windage Areas	SA	Sail Area
C_D, C_L	Drag & Lift Coefficients	SpanEff	Effective Span
C_X	Driving Force Coefficient	SpanRef	Reference Span
C_Y	Heeling Force Coefficient	TWA	True Wind Angle
CE	Centre of Effort	TWS	True Wind Speed
CEA	Centre of Effort Aft of Ref. Point	VPP	Velocity Prediction Program
D, L	Drag & Lift Force Vectors	xCE	Longitudinal Centre of Effort
DOF	Degree of Freedom	zCE	Vertical Centre of Effort
DWL	Design Waterline		
F_{DRIVE}	Driving Force		

1. INTRODUCTION

Wind tunnel testing has been extensively used over the years to predict and refine the performance of sailing yacht sail plans – being a particularly efficient tool for evaluating forces and centres of effort of detailed models with complex rig arrangements and sail combinations. Significant research on the investigation of sail plans aerodynamics has been published by Marchaj (1979, 1982, 2003), Claughton (1994), Campbell (1997, 1998), Ranzenbach (1997, 2002), Le Pelley (2002), to mention only a few.

Yacht rigs and sails aerodynamic research and performance evaluation have been conducted at the University of Southampton's wind tunnels since the early 1960s by the Yacht Research Group (S.U.Y.R.) and Advisory Committee (A.C.Y.R.) – e.g. Marchaj (1962, 1964, 1974, 1978) and Tanner (1968) – and, since its inception in 1967, by the Wolfson Unit MTIA, covering all rig and vessel types, incl. sloops, ketches and schooners, square riggers, DynaRigs and wind assisted technologies.

This paper describes wind tunnel tests carried out at the Wolfson Unit on a scale model of the 68m ketch *Project Zero*. The tests were conducted with the aim of evaluating the performance of sailplan options across a range of upwind, offwind and reefed configurations and the effects of sail settings upon longitudinal centre of effort location with various sail combinations.

VPP aerodynamic models of various configurations have been created to enable the performance of each to be evaluated when the yachts stability and hydrodynamic characteristics are taken into account. This data enables the vessel's performance to be evaluated along with yaw and rudder balance across a range of wind speeds and directions. Finally, some of the aspects of how the wind tunnel data have been used are also addressed in this paper.

2. BACKGROUND

2.1. Aerodynamic Forces

A schematic diagram of the aerodynamic force components acting on a ketch-rigged sailing yacht is presented in Figure 1, with the forces decomposed in the boat's course coordinate system. The total aerodynamic force is assumed to act through the centre of effort CE, as explained by Marchaj (1974, 1979) and Claughton (1998).
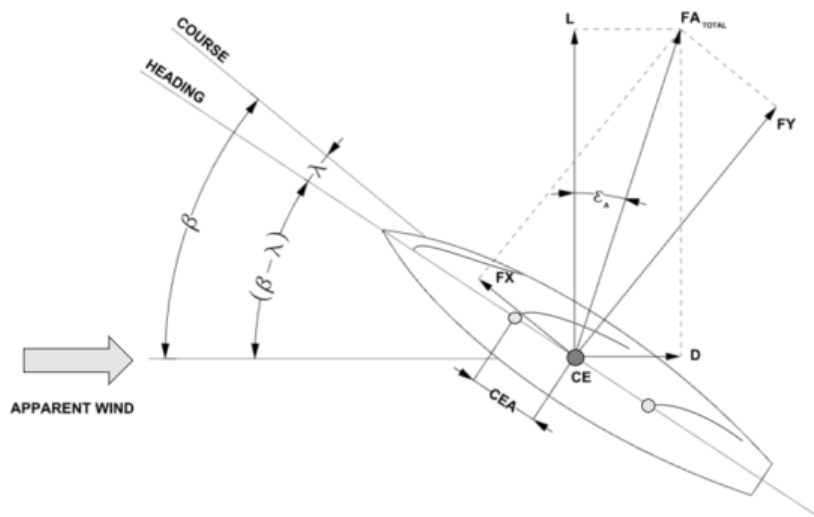

Figure 1. Aerodynamic Forces on a Ketch-Rigged Sailing Yacht – Schematic Diagram.

2.2. *Project Zero* Sailing Yacht

The zero-fossil-fuel *Project Zero* is the centrepiece of the *Foundation Zero* mission, developed by a group of impact investors in collaboration with Dykstra Naval Architects, among other technical partners. *Project Zero* is a 68m ketch with the principal dimensions listed in Table 1. The vessel's sail plan is presented in Figure 2 with the list of sails tested and their areas listed in Table 2.
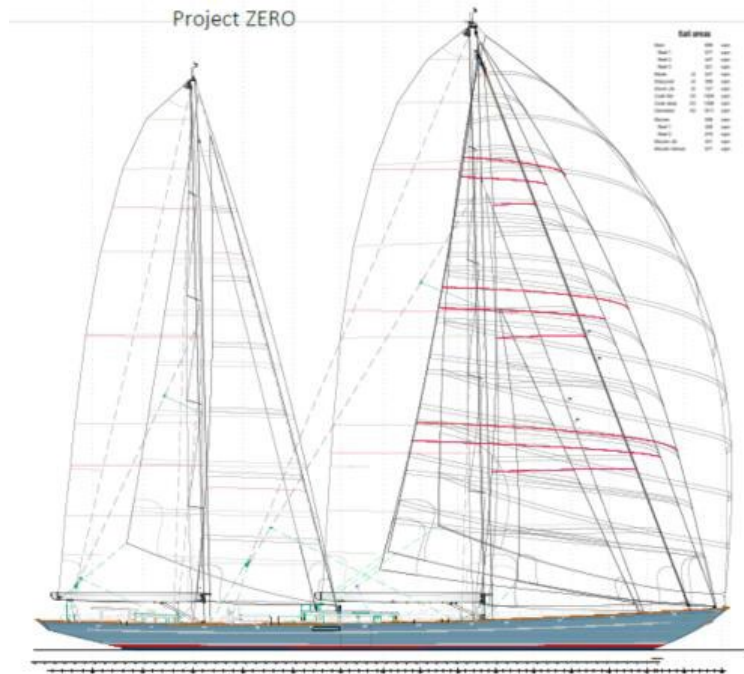

Figure 2. *Project Zero* – Sail Plan.

Table 1. Principal Dimensions and Reference Values.

Parameter	Value	Unit
LOA	68	m
LWL	51.28	m
BWL	10.01	m
Tc	1.96	m
Tmax	8.4	m
Displacement	450	tonnes
Reference Span (Mast Height)	62.20	m
Reference Waterline Length	51.28	m
Vertical Reference	DWL	
Longitudinal Reference	Main Mast CL	

Table 2. List of Sails Tested and Sail Areas.

Sail	Code	Area (m²)
Mainsail	Mn	698
Main Reef 1	RMn1	577
Main Reef 2	RMn2	447
Main Reef 3	RMn3	321
Blade	B	537
Staysail	Ss	309
Storm Jib	SJ	157
Code 0	C0	1030
A3	A3	1308
AP Gennaker	A2	1811
Mizzen	Mz	556
Mizzen Reef 1	RMz1	426
Mizzen Reef 2	RMz2	279
Mizzen Jib	MzJ	331
Mizzen Staysail	MzSs	577

2.3. Design Considerations

What makes *Project Zero* stand out from other sailing yachts of this size is that there will be no fossil fuels on board. No engines, no generator sets, no range extenders, only batteries. The foreseen battery capacity is 5 MWh (the energetic equivalent of 900 litres of Marine Diesel Oil) and the batteries can be replenished on board, e.g. using energy harvested from the sun and wind.

The primary means of harvesting energy when under way is by using hydro-generation. Not uncommon nowadays on ocean-going yachts, but the extent to which *Project Zero* relies on that source of energy is evident, since this energy is not only needed to power the hotel load and navigational systems, but also to motor assist through light wind patches.

The rig and sailplan were designed with the aim to perform adequately in both upwind and downwind conditions as the yacht would need to sail all the time, i.e. across a wide range of wind directions; with an emphasis on the high gain reaching angles at which hydro-generation would be most beneficial. This consideration led to a relatively low, but powerful rig, with a cascade of sails to maximise the lift generating capabilities. Combined with sleek lines and ample stability from a deep keel, this struck the optimal balance for *Zero* to sail across the oceans in total energy autonomy.

A second consideration for the rig design was that in heavy weather conditions, this yacht would not have the option to strike the sails and motor through. Therefore, a particular attention was given towards the design of a well-balanced and performant reef plan.

3. MODEL

1:35 scale model hull, superstructure, masts and booms were constructed by the Wolfson Unit in accordance with drawings supplied by Dykstra Naval Architects. The model sails were designed by Doyle Sails NZ and manufactured by Doyle Sails UK. The masts rake and pre-bend were set to match the design and the rigging tension was set to control the masts deflection under wind loading.

A remote-control sail winch system was used to trim all the sails; the mizzen and main were sheeted using a bridle style mainsheet arrangement with a vang being employed at the reaching and offwind angles. All other sails were sheeted with mechanisms broadly duplicating the as designed configurations and sheeting positions. The A2 was rigged with an adjustable tackline remotely controlled. Figure 3 shows the model rigged with the sail configuration #1 under tests at 25° AWA.
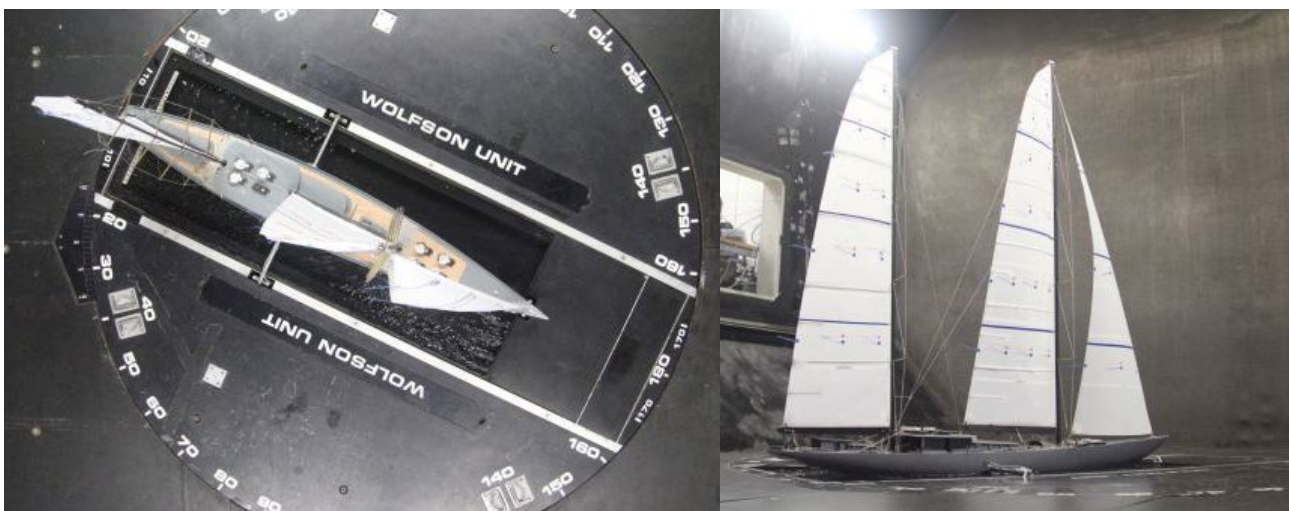

Figure 3. Model in the wind tunnel (sail configuration #1 – upwind, AWA 25°).

4. TEST ARRANGEMENT

4.1. Wind Tunnel

The tests were conducted at the University of Southampton in the low-speed section of the No.1 Wind Tunnel, which has dimensions 4.6m wide by 3.7m high. The model was mounted upright on a six-component balance (Figure 4) which was attached to a 2.6m turntable such that measured forces were in the boat axis system. The model was suspended from the balance in a tank of water, fitted into the turntable, which provided a seal between the model and the turntable and permitted the measurement of the model forces independent of the turntable.
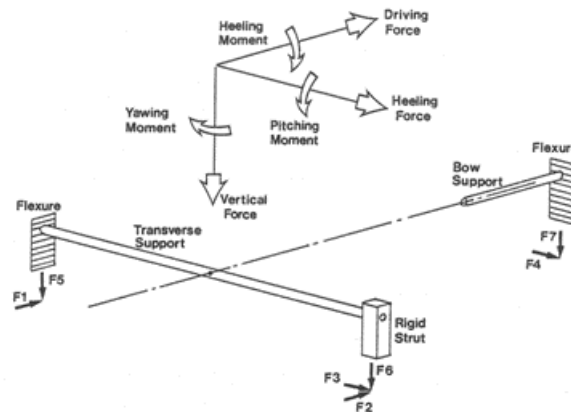

Figure 4. Dynamometer Force Balance – Schematic Arrangement.

4.2. Test Procedure

For each sail combination at each tested apparent wind angle the sail trims were optimised to produce the maximum driving force. Having achieved this, other combinations of sheeting were tested, to simulate sail sets that were appropriate to a de-powered mode, i.e. maximum drive at a specified limit of heeling moment or force. In the case of upwind apparent wind angles, a number of runs are needed to clearly define the eased settings, whereas for the offwind apparent wind angles this is not necessary.

4.3. Wind Speed

During wind tunnel sail tests, the wind speed is chosen to match the load capacity of the dynamometer and to avoid structural problems with the model, sheeting system and winches, whilst maximising the forces measured and resolution. The majority of the "white sails" configurations tests were carried out at a dynamic pressure (q) of 29.4 Pascals, which corresponds to a wind speed of approximately 6.9 m/s. The offwind sail configurations tests were carried out at a dynamic pressure (q) of 14.7 Pascals, which corresponds to a wind speed of approximately 4.9 m/s.

As explained by Campbell (1998) and Claughton (1994, 1998), the wind speed usually used for offwind sail tests in the No.1 Wind Tunnel is approximately 5 m/s. This wind speed also gives a good match to the full-scale flying shapes of downwind sails.

4.4. Flow Turbulence

In order to produce a uniform airflow, fine mesh screens are placed immediately upstream of the model. They also have the beneficial effect of introducing fine scale turbulence into the airflow, which increases the effective Re and hence improves the modelling of shear layers in leading edge separation bubbles and the trailing edge separation points (Claughton, 1994 and Campbell, 1998).

5. TEST RESULTS

A summary of the tests is presented in Table 3 which contains the apparent wind angles for the various sail configurations tested.

Table 3. Tests Summary.

Test series no.	Configuration	Mn (Main)	RMn1 (Main Reef 1)	RMn2 (Main Reef 2)	RMn3 (Main Reef 3)	B (Blade)	Ss (Staysail)	SJ (Storm Jib)	C0 (Code 0)	A3	A2 (AP Gennaker)	Mz (Mizzen)	RMz1 (Mizzen Reef 1)	RMz2 (Mizzen Reef 2)	MzJ (Mizzen Jib)	MzSs (Mizzen Staysall)	Apparent wind angle
1 - 2	1	X				X						X					30
3	1	X				X						X					35
4 - 5	1	X				X						X					25
6 - 8	1	X				X						X					20
9	1	X				X						X					45
10	1	X				X						X					60
11	1	X				X						X					90
12	1	X				X						X					60
13	2	X				X						X			X		60
14	2	X				X						X					45
15	2	X				X						X					35
16 - 17	3	X							X			X					60
18 - 19	3	X							X			X					45
20 - 21	3	X							X			X					75
22	4	X								X		X					75
23	4	X								X		X					60
24	4	X								X		X					45
25 - 26	5	X								X		X				X	60
27 - 28	5	X								X		X				X	75
29 - 30	5	X								X		X				X	90
31	5	X									X	X				X	120
32	6	X							X			X				X	60
33	6	X							X			X					75
34	6	X							X			X					90
35	7										X	X				X	60
36	7										X	X					75
37	7										X	X					90
38	7										X	X					120
39	8										X						120
40	8										X						90
41	9	X				X							X				30
42 - 43	9	X				X							X				35
44 - 46	9	X				X							X				45
47	9	X				X							X				60
48 - 49	10	X					X							X			35
50	10	X					X								X		45
51	11			X			X										35
52	11			X			X										45
53	11			X			X										60
54	12				X			X									45
55	12				X			X									35
56	--																Windage

6. DATA ANALYSIS

6.1. Data Reduction

The measured forces were corrected for "end zeroes", transformed to lift and drag coefficients (C_L & C_D) with standard tunnel corrections applied, including wall correction to wind angle & C_D and wake blockage correction to C_L & C_D due to the influence of separated flow.

The data were analysed in three ways:

6.1.1. Force Coefficients

Firstly, in the conventional manner, by non-dimensionalising the sail forces on the basis of the total sail area for each configuration, and the mean dynamic pressure (q) in the wind tunnel.

6.1.2. Forces at Unity Wind Pressure

Secondly, the forces were analysed to determine the driving and heeling forces and the heeling moment produced by the hull and sails, at unity wind pressure.

6.1.3. VPP Input Files

Thirdly, for VPP calculations faired sets of lift and drag coefficients and associated centre of effort heights were fitted to the corrected values and the associated values of driving force and heeling moment were calculated for comparison.

6.2. Data Fits for VPP Calculations

Sail coefficients can be input into VPP programs, such as the WinDesign VPP developed by Oliver (1995) as *.AEX aerodynamic experimental sailset files. The data required are:

- maximum lift (C_L) and drag (C_D) coefficients,
- centre of effort height (Z_{CE}) and effective span (SpanEff) expressed as a percentage of the mast height/span reference (SpanRef) at specified apparent wind angles,
- the sail area and reduction of centre of effort coefficient ($Z_{CE(reduced)}$ factor).

The effective span is for induced drag reductions at lower lift coefficients and $Z_{CE(reduced)}$ factor is for calculation of centre of effort height at reduced lift coefficient.

Fair curves are required by the VPP for the variation of lift and drag coefficients with apparent wind angle, in order for the VPP to interpolate values and iterate to a solution. The curves were faired by manual adjustment to the fitted coefficients, which are shown plotted on the various charts, and the coefficients are presented in Appendix Table A1. The driving force and heeling moment values were computed from the windage and sail coefficients using the effective rig height and centre of effort height.

6.3. Windage Forces and Coefficients

Windage tests were carried out on the hull and superstructure, masts and booms (with all sails removed and booms on centreline). A fit using the windage algorithms in the WinDesign VPP was produced using a frontal (Ax) and lateral (Ay) windage areas, based on drag coefficients of $C_D = 1$, Ax = 118 m^2 and Ay = 300 m^2. The VPP windage function does not completely encapsulate the actual measured data across the entire apparent wind range. This results in a small component of windage remaining in the sail coefficients, which when re-combined with the VPP windage still results in the same total driving and heeling forces/moments measured in the tunnel.

The windage forces were subtracted from the total forces to yield the sail coefficients excluding windage. These have been normalised using configuration #1 (Mn + B + Mz) giving a total sail area of 1791 m^2 for comparison with the sail coefficients.

An average centre of effort height from the heel moments due to windage were subtracted from the total measured moments. It is therefore implicit that this value (22.8%, 14.18m above DWL) should be used in the VPP. Care must be taken in the VPP inputs as windage is usually referenced within VPP programs to the height of base of I (HBI). It is advisable to use windage and sail coefficients as separate inputs into VPP calculations to ensure that reefing calculations are correctly performed.

6.4. Drag Coefficient versus Lift Coefficient Squared (Cd vs Cl^2) Chart

The data plotted in Figure 5 was derived from the sail forces excluding windage, for the upwind conditions. By plotting the data as lift and drag coefficients for upwind sail settings, various components of drag can be identified. These are required in order to apply boundary corrections to the wind tunnel data and for input into a VPP program, to predict the sailing performance of the yacht using the wind tunnel data, but may also be studied in order to investigate the efficiency of the rig.

Appendix Figures A1b to A5b show the results for all the various sail configurations separately tested at a range of apparent wind angles from 20° to 120°. A number of the corresponding VPP fits are also shown.
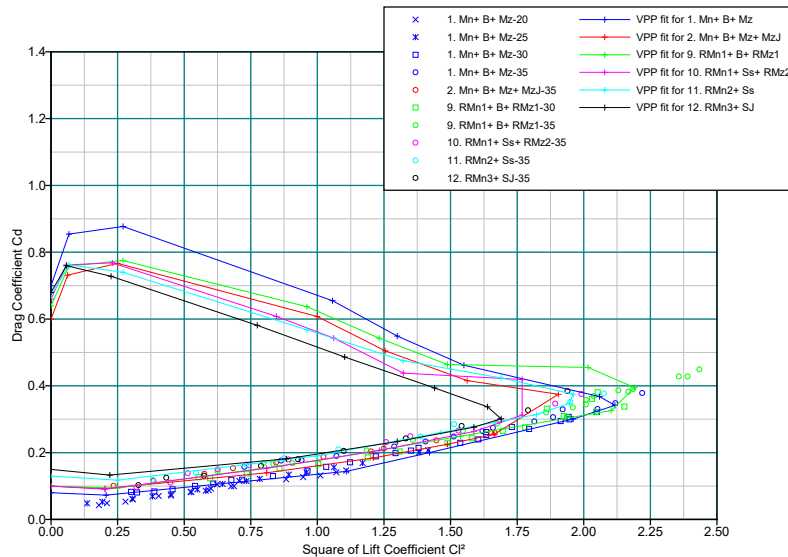
Figure 5. Chart of Cd vs Cl^2 – Upwind.

6.5. Centre of Effort Charts

The lower diagram of Figure 6 shows the vertical position of the centre of effort (CEH) of the rig for the upwind conditions, derived from the heeling forces and the resultant of the roll and pitch moment measurements, plotted against heeling force coefficient. The centre of effort height is referenced to the waterline and is expressed as a percentage of the mast height above DWL, which was taken as 62.2m. The upper diagram shows the longitudinal position of the centre of effort, derived from driving force, heeling force and yaw moment measurements. The position is referenced to the main mast centreline, and is expressed as a percentage of the waterline length, which was taken as 51.28m.

The CEH and CEA positions for all the conditions are presented in Appendix Figures A1d to A5d.
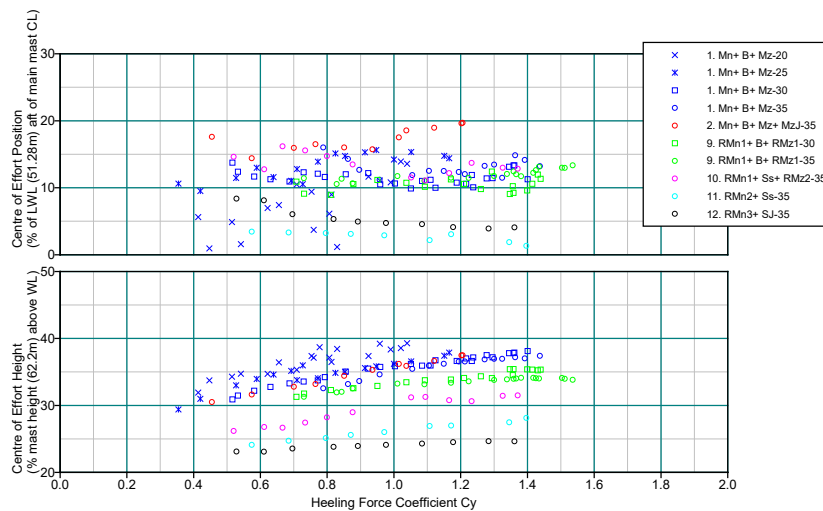
Figure 6. Chart of Centre of Effort – Upwind.

6.6. Lift and Drag Coefficients

The variation of lift and drag coefficient with apparent wind angle for each sail configurations have not been presented graphically in this paper but are listed in the aerodynamic VPP input data files (Appendix Table A1).

8

The data fits for VPP calculations do not necessarily encompass the maximum values of lift and drag, since some of these were obtained with the sails over sheeted. Instead, the fit was made to encompass the maximum driving force achieved at each angle. The data fits were extrapolated to lower and higher apparent wind angles than those used for the tests. This was to aid the curve fairing and to enable the VPP to iterate to values within the range of test data. Attempts were made to reduce lift and increase drag in the extrapolated ranges so the VPP would produce pessimistic performance predictions at apparent wind angles outside the range of test values.

6.7. Driving Force versus Heeling Moment Charts

Figure 7 contains the variation of driving force versus heeling moment at unity wind pressure derived from the corrected sail coefficients including windage, for the boat upright at various apparent wind angles, for the upwind conditions. Appendix Figures A1c to A5c show the results for all the conditions tested. These plots were used to verify the fit of the derived VPP sail coefficients to the experimental data and show the relative performance of different sail configurations. The relative performance of different sail combinations can be assessed for light wind conditions by comparing the maximum values of driving force at a particular apparent wind angle. For medium and strong wind conditions the values of driving force at reduced values of heeling moment may be compared.
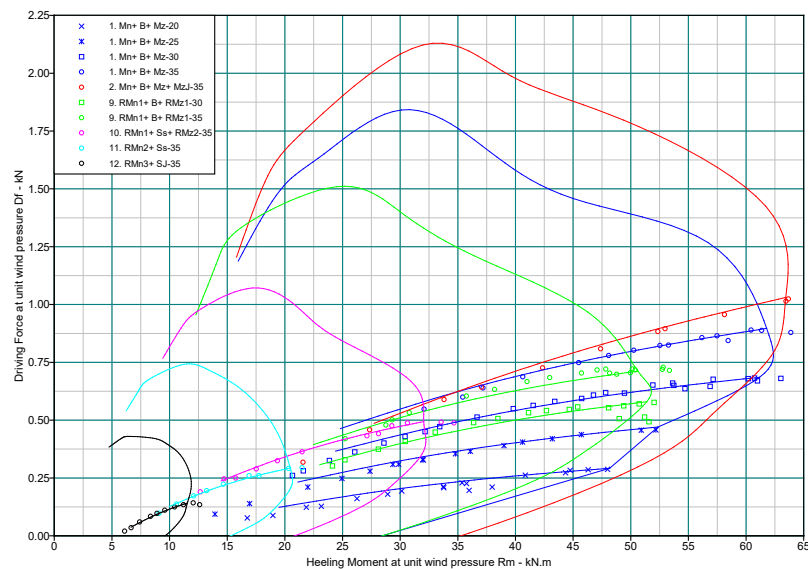
Figure 7. Chart of Driving Force vs Heeling Moment – Upwind.

7. DISCUSSION OF RESULTS AND GENERAL REMARKS

It can be seen from Table 3 that a number of different sail combinations were tested at various apparent wind angles and generally the tests included progressively easing the sheets to de-power the rig. The results have been grouped together for presentation in the figures (Appendix A1 to A5), as follows: upwind, downwind, reefed configurations, Blade & Mizzen Jib use and Code 0 & A3 use. The reader may still have to examine the data from several figures in this paper in order to compare the performance of different sails. The experimental data was consistent between data sets and allowed a smoothly varying VPP fit, indicating low uncertainty and good reliability within the data.

A more complete description of the performance of each sailset can be gained by inputting the VPP files listed in Appendix Table A1 into the WinDesign VPP and combining them with hydrodynamic properties (including stability) to estimate the boat speeds and heel angles at a range of true wind speeds and angles. The CEA information can be combined with the hydrodynamically derived centre of lateral resistance (CLR) data to predict steady state sailing rudder angles, and the aero force vector information can be used within a VPP using yaw balance (M_{YAW}). For example, such a method is presented by Prince et al (2013).

8. USE OF THE WIND TUNNEL DATA

The wind tunnel data fits were augmented with the measured longitudinal centre of effort information for all the tested sailsets. In the specific case of *Project Zero*, this aerodynamic performance information was used in a VPP developed by Dykstra Naval Architects (DNA) that solves the equations of motion in 4 degrees of freedom (F_X, F_Y, M_{ROLL}, M_{YAW}).

The DNA VPP requires hydrodynamic input from CFD calculations or towing tank tests, and it allows for a hydro-generator to be modelled in the force equilibrium. Figure 8 shows the predicted performance for a selection of sailsets at combinations of true wind speed and angle in flat water, with the power yield of the hydro-generators displayed on the lower vertical axis. The maximum yield of the hydro-generators is predicted to be ~250 kW at 18 knots TWS, 120° TWA with sail configuration #4 (Mn + A3 + Mz + MzJ).
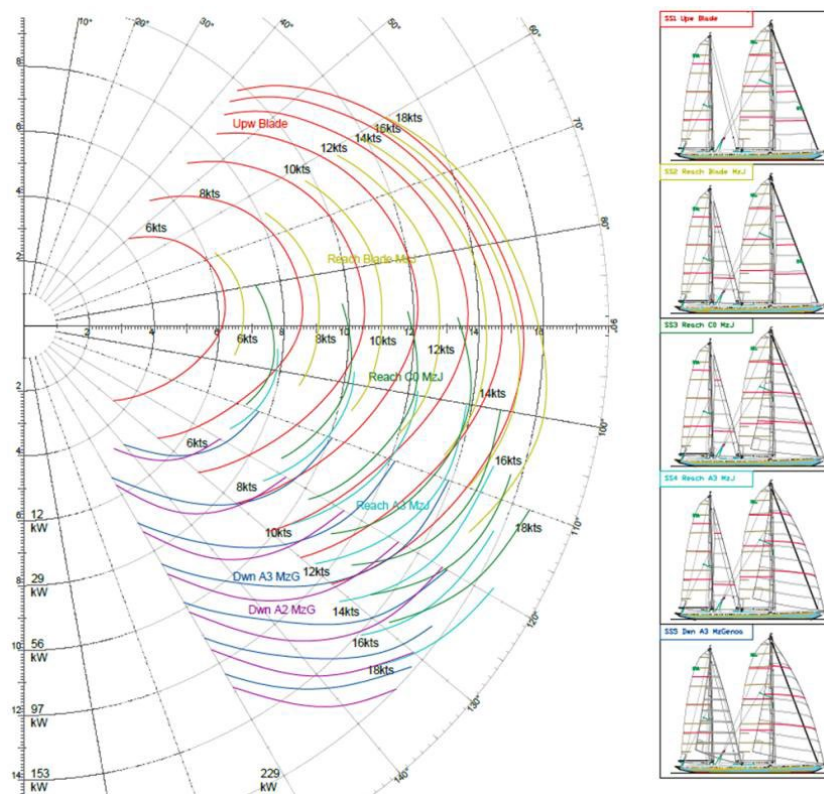
Figure 8. *Project Zero* **– Predicted Speed Polar Diagram with Hydro-Generation.**

Using the velocity and power predictions outcomes, routing analyses based on historical weather data were performed to predict the ability of the yacht to perform long crossings in acceptable time.

In recent years, Dykstra Naval Architects have gathered on-water data and compared them to VPP predictions, to help validate the prediction methods. This was done for several yachts, both with the DNA in-house VPP (using wind tunnel tests as the aerodynamic model), and with the 2020 ORC VPP (using the ORC aerodynamic formulations). As an example, the predicted vs on-water boatspeeds difference for the 67m ketch *Hetairos* are presented in Figure 9 for both VPPs as a percentage of the on-water boatspeed. The differences observed upwind can partly be attributed to the added resistance in waves that was not accounted for in the VPP results presented.

Over the years, Dykstra Naval Architects have observed a significant improvement in performance prediction accuracy when using wind tunnel data relative to empirical or CFD generated data, especially for multi-masted cruising rigs. This, combined with the added insight in the sail handling, sheeting arrangements, and flow interaction between the hull, superstructures and sails, highlights that wind tunnel testing remains a very valuable design tool in the current day and age.
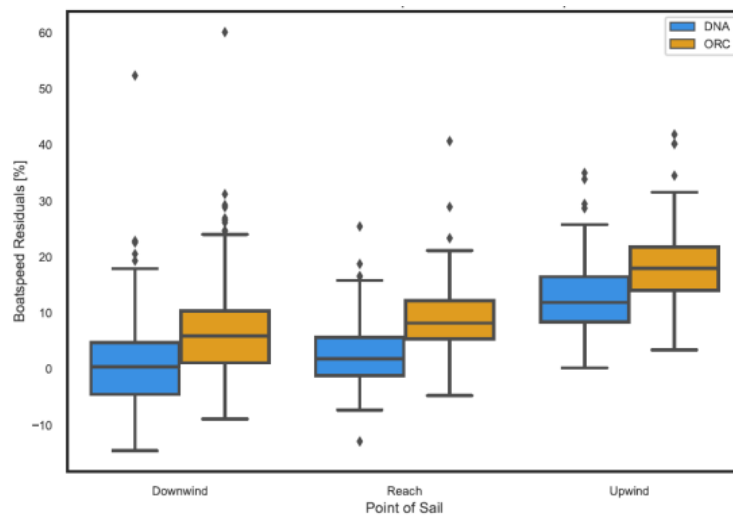
Figure 9. *Hetairos* **– DNA VPP & ORC VPP Comparison as % of On-water Boatspeed.**

9. CONCLUSIONS

This paper presented wind tunnel tests carried out on a scale model of the 68m ketch *Project Zero*. A comprehensive aerodynamic dataset of the yacht's sailsets was presented. The performance of sailplan options across a range of upwind, offwind and reefed configurations and the effects of sail settings upon longitudinal centre of effort location with various sail combinations were evaluated.

VPP aerodynamic models of various configurations were created to enable the performance of each to be evaluated when the yachts stability and hydrodynamic characteristics are taken into account, enabling the evaluation of the vessel's performance and rudder balance across a range of wind speeds and directions. These models were subsequently used to assess the ability of the yacht to harvest energy by means of hydro-generation as well as to perform routing analyses.

The data presented in this paper can be used by yacht designers and researchers to help validate and even refine their numerical tools and to offer a starting point values in the absence of other data sources.

Finally, it can be seen from this paper that wind tunnel testing is a particularly efficient tool for evaluating forces and centres of effort of sailing vessels with complex rig arrangements and sails combinations in a timely and practical manner, allowing for a large range of configurations and trim settings to be evaluated, as well as the possibility to make observations and adjustments ad-hoc.

10. ACKNOWLEDGEMENTS

11. REFERENCES

Campbell, I.M.C. (1998). The performance of offwind sails obtained from wind tunnel tests. Intl Conf on "The Modern Yacht".

Campbell, I.M.C. (1997). Optimisation of a sailing rig using wind tunnel data. The Thirteenth Chesapeake Sailing Yacht Symposium, SNAME, Annapolis.

Claughton, A.R., Wellicome, J.F., Shenoi, R.A. (1998). *Sailing Yacht Design: Theory*.

Claughton, A.R., Campbell, I.M.C. (1994). Wind tunnel testing of sailing yacht rigs. 13th HISWA Intl Symp on "Yacht Design and Yacht Construction".

Le Pelley, D., Ekblom, P., Flay, R. (2002). Wind Tunnel Testing of Downwind Sails. The 1st International Conference on High Performance Yacht Design, Auckland.

Marchaj, C.A. (2003). *Sail Performance.*

Marchaj, C.A. (1982). *Sailing Theory and Practice*.

Marchaj, C.A. (1979). *Aero-Hydrodynamics of Sailing*.

Marchaj, C.A. (1978). A critical review of methods of establishing sail coefficients and their practical implications in sailing and in performance prediction. Wolfson Marine Craft Symposium, University of Southampton.

Marchaj, C.A. (1974). Rig Development Tests of a 1/16.6 Scale Model of an 80ft Cruising Ketch. S.U.Y.R. Report No. 36.

Marchaj, C.A., Tanner, T. (1964). Wind Tunnel Tests of a 1/4 Scale Dragon Rig. S.U.Y.R. Technical Note No. 14.

Marchaj, C.A. (1964). The Aerodynamic Characteristics of a 2/5th scale "Finn" Sail and its Efficiency when Sailing to Windward. A.C.Y.R. Report No. 13.

Marchaj, C.A. (1962). Wind Tunnel Tests of a 1/3rd Scale Model of an X-One Design Yacht's Sails. S.U.Y.R. Report No. 11.

Oliver, J.C. & Claughton, A.R. (1995). Development of a Multi-Functional Velocity Prediction Program (VPP) for Sailing Yachts. R.I.N.A. International Conference CADAP '95: Computer-Aided Design and Production for Small Craft, Southampton, September.

Prince, M. & Claughton, A.R. (2013). Estimating a Yacht's Hull-Sailplan Balance and Sailing Performance Using Experimental Results and VPP Methods. INNOVSAIL 3rd Edition International Conference on Innovation in High Performance Sailing Yachts, Lorient.

Ranzenbach, R., Teeters, J. (2002). Enhanced depowering model for offwind sails. The 1st International Conference on High Performance Yacht Design, Auckland.

Ranzenbach, R., Mairs, C. (1997). Experimental determination of Sail performance and blockage corrections. The Thirteenth Chesapeake Sailing Yacht Symposium, SNAME, Annapolis.

Tanner, T. (1968). The Analysis of Wind Tunnel Data. S.U.Y.R. Technical Note No. 503.

12. APPENDIX

Table A1. Aerodynamic VPP input files (*.AEX).

Sail Configuration
AreaRef Base Ht. SpanRef $Z_{CE\ (reduced)}$ factor
No. of AWA
AWA C_L C_D $Z_{CE\ (ratio)}$ SpanEff $_{(ratio)}$

1. Mn+ B+ Mz

AWA	C_L	C_D	$Z_{CE\ (ratio)}$	SpanEff$_{(ratio)}$
1791.000	0.00	62.200	0.784	
13				
0.00	0.0000	0.0800	0.4042	1.1576
10.00	0.4550	0.0728	0.4042	1.1576
20.00	1.0530	0.1439	0.4042	1.1576
25.00	1.1920	0.2002	0.3901	1.0932
30.00	1.4000	0.3005	0.3894	1.0450
35.00	1.4550	0.3417	0.3844	1.0450
45.00	1.4350	0.3679	0.3788	1.0450
60.00	1.2450	0.4618	0.3638	0.8360
75.00	1.1400	0.5490	0.3602	0.8360
90.00	1.0280	0.6548	0.3565	0.8360
120.00	0.5200	0.8770	0.3565	0.8360
135.00	0.2600	0.8543	0.3565	0.8360
150.00	0.0000	0.7000	0.3565	0.8360

2. Mn+ B+ Mz+ MzJ

AWA	C_L	C_D	$Z_{CE\ (ratio)}$	SpanEff$_{(ratio)}$
2122.000	0.00	62.200	0.840	
13				
0.00	0.0000	0.1000	0.4048	1.2540
10.00	0.4500	0.0925	0.4048	1.2540
20.00	0.9000	0.1399	0.4048	1.2540
25.00	1.1000	0.1843	0.3900	1.2540
30.00	1.2200	0.2252	0.3897	1.2540
35.00	1.2900	0.2548	0.3848	1.2540
45.00	1.3800	0.3745	0.3591	1.0450
60.00	1.2500	0.4158	0.3525	1.0130
75.00	1.1200	0.5052	0.3473	0.9650
90.00	1.0000	0.6075	0.3473	0.9650
120.00	0.5000	0.7669	0.3473	0.9650
135.00	0.2500	0.7317	0.3473	0.9650
150.00	0.0000	0.6000	0.3473	0.9650

3. Mn+ C0+ Mz+ MzJ

AWA	C_L	C_D	$Z_{CE\ (ratio)}$	SpanEff$_{(ratio)}$
2615.000	0.00	62.200	0.939	
13				
0.00	0.0000	0.1500	0.4209	1.2220
10.00	0.4250	0.1460	0.4209	1.2220
20.00	0.8500	0.1941	0.4209	1.2220
25.00	1.0500	0.2388	0.4209	1.2220
30.00	1.2000	0.2875	0.4183	1.2220
35.00	1.3400	0.3437	0.4157	1.2220
45.00	1.5150	0.4407	0.4085	1.2220
60.00	1.4800	0.6318	0.3887	0.9000
75.00	1.2450	0.8526	0.3789	0.8680
90.00	1.0000	0.9556	0.3726	0.8680
120.00	0.5000	1.0114	0.3674	0.8680
135.00	0.2500	0.9778	0.3674	0.8680
150.00	0.0000	0.8000	0.3674	0.8680

4. Mn+ A3+ Mz+ MzJ

AWA	C_L	C_D	$Z_{CE\ (ratio)}$	SpanEff$_{(ratio)}$
2893.000	0.00	62.200	0.956	
13				
0.00	0.0000	0.1500	0.4301	1.1580
10.00	0.4250	0.1521	0.4301	1.1580
20.00	0.8500	0.2132	0.4301	1.1580
25.00	1.0500	0.2707	0.4301	1.1580
30.00	1.2000	0.3206	0.4301	1.1580
35.00	1.3400	0.3837	0.4301	1.1580
45.00	1.5300	0.5005	0.4250	1.1580
60.00	1.4900	0.6316	0.4121	0.9970
75.00	1.3900	0.8214	0.3809	0.8040
90.00	1.1500	0.9270	0.3727	0.8040
120.00	0.6000	0.9626	0.3654	0.8040
135.00	0.3000	0.9331	0.3654	0.8040
150.00	0.0000	0.7600	0.3654	0.8040

5. Mn+ A3+ Mz+ MzSs

AWA	C_L	C_D	$Z_{CE\ (ratio)}$	SpanEff$_{(ratio)}$
3139.000	0.00	62.200	1.012	
13				
0.00	0.0000	0.1500	0.4308	1.1580
10.00	0.4250	0.1548	0.4308	1.1580
20.00	0.8500	0.2191	0.4308	1.1580
25.00	1.0500	0.2873	0.4308	1.1580
30.00	1.2000	0.3523	0.4308	1.1580
35.00	1.3200	0.4221	0.4308	1.0450
45.00	1.5000	0.5321	0.4257	1.0450
60.00	1.5500	0.6382	0.4102	1.0450
75.00	1.5000	0.8113	0.3803	0.8680
90.00	1.2400	0.8471	0.3682	0.8680
120.00	0.7600	0.7680	0.3338	0.8680
135.00	0.4000	0.7148	0.3338	0.8680
150.00	0.0000	0.5600	0.3338	0.8680

6. Mn+ C0+ Mz+ MzSs

AWA	C_L	C_D	$Z_{CE\ (ratio)}$	SpanEff$_{(ratio)}$
2861.000	0.00	62.200	1.037	
13				
0.00	0.0000	0.1500	0.4323	1.1580
10.00	0.4250	0.1517	0.4323	1.1580
20.00	0.8500	0.2068	0.4323	1.1580
25.00	1.0500	0.2685	0.4323	1.1580
30.00	1.2000	0.3328	0.4323	1.1580
35.00	1.3000	0.3943	0.4323	1.0450
45.00	1.4300	0.4908	0.4272	1.0450
60.00	1.4600	0.5976	0.3930	0.9320
75.00	1.3300	0.7686	0.3817	0.7720
90.00	1.1800	0.8299	0.3741	0.7720
120.00	0.7200	0.7747	0.3323	0.7720
135.00	0.3700	0.7241	0.3323	0.7720
150.00	0.0000	0.5800	0.3323	0.7720

7. Mn+ A2+ Mz+ MzSs

3642.000	0.00	62.200	0.999	
13				
0.00	0.0000	0.1600	0.4466	1.1580
10.00	0.3000	0.1601	0.4466	1.1580
20.00	0.6000	0.1904	0.4466	1.1580
25.00	0.7500	0.2257	0.4466	1.1580
30.00	0.9000	0.2810	0.4466	1.1580
35.00	1.0000	0.3244	0.4466	1.0450
45.00	1.1500	0.4129	0.4466	1.0450
60.00	1.2900	0.5366	0.4259	1.0450
75.00	1.4000	0.7107	0.4063	0.9650
90.00	1.1900	0.7232	0.3899	0.8680
120.00	0.7100	0.7305	0.3761	0.8680
135.00	0.4000	0.6836	0.3708	0.8680
150.00	0.0000	0.5200	0.3708	0.8680

8. Mn+ A2+ Mz

3065.000	0.00	62.200	1.022	
13				
0.00	0.0000	0.1600	0.4543	1.1580
10.00	0.3000	0.1569	0.4543	1.1580
20.00	0.6000	0.1777	0.4543	1.1580
25.00	0.7300	0.2102	0.4543	1.1580
30.00	0.8500	0.2459	0.4543	1.1580
35.00	0.9500	0.2884	0.4543	1.0450
45.00	1.1000	0.3994	0.4490	1.0450
60.00	1.2200	0.5337	0.4333	1.0450
75.00	1.2600	0.6799	0.4123	0.9650
90.00	1.1000	0.7250	0.3913	0.8680
120.00	0.7000	0.7840	0.3989	0.8680
135.00	0.4000	0.7536	0.3936	0.8680
150.00	0.0000	0.6000	0.3936	0.8680

9. RMn1+ B+ RMz1

1540.000	0.00	62.200	0.882	
13				
0.00	0.0000	0.1000	0.3836	0.9650
10.00	0.5000	0.0940	0.3836	0.9650
20.00	1.0000	0.1761	0.3805	0.9650
25.00	1.2400	0.2492	0.3733	0.9650
30.00	1.4500	0.3261	0.3630	0.9650
35.00	1.4800	0.3951	0.3501	0.8840
45.00	1.4200	0.4552	0.3415	0.8040
60.00	1.2200	0.4639	0.3390	0.6750
75.00	1.1100	0.5426	0.3338	0.6750
90.00	0.9800	0.6371	0.3338	0.6750
120.00	0.5200	0.7752	0.3338	0.6750
135.00	0.2600	0.7588	0.3338	0.6750
150.00	0.0000	0.6400	0.3338	0.6750

10. RMn1+ Ss+ RMz2

1165.000	0.00	62.200	0.848	
13				
0.00	0.0000	0.1000	0.3641	0.9650
10.00	0.4500	0.0908	0.3641	0.9650
20.00	0.9000	0.1534	0.3589	0.9650
25.00	1.1100	0.2068	0.3486	0.9650
30.00	1.2600	0.2634	0.3383	0.9650
35.00	1.3300	0.3123	0.3229	0.8040
45.00	1.3300	0.4192	0.3131	0.7070
60.00	1.1500	0.4382	0.3080	0.6750
75.00	1.0300	0.5432	0.3080	0.6750
90.00	0.9200	0.6081	0.3080	0.6750
120.00	0.4800	0.7685	0.3080	0.6750
135.00	0.2400	0.7621	0.3080	0.6750
150.00	0.0000	0.6600	0.3080	0.6750

11. RMn2+ Ss

756.000	0.00	62.200	0.875	
13				
0.00	0.0000	0.1300	0.3053	0.6430
10.00	0.5000	0.1176	0.3053	0.6430
20.00	1.0000	0.1904	0.3053	0.6430
25.00	1.2100	0.2603	0.3002	0.6430
30.00	1.3500	0.3142	0.2951	0.6430
35.00	1.3950	0.3478	0.2869	0.6430
45.00	1.4000	0.3749	0.2752	0.6430
60.00	1.3000	0.4236	0.2656	0.5790
75.00	1.1500	0.4754	0.2656	0.5790
90.00	0.9800	0.5682	0.2656	0.5790
120.00	0.5200	0.7402	0.2656	0.5790
135.00	0.2600	0.7625	0.2656	0.5790
150.00	0.0000	0.6700	0.2656	0.5790

12. RMn3+ SJ

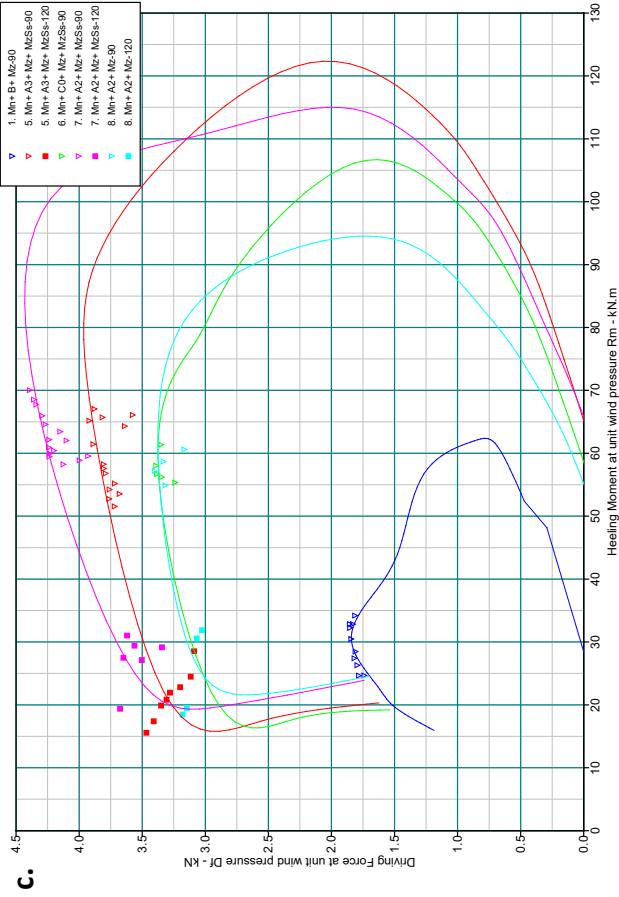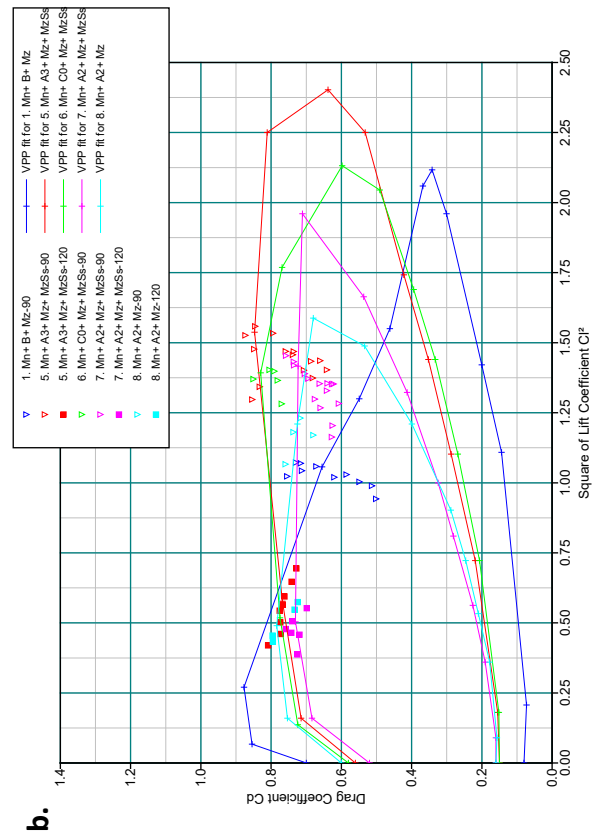| 478.000	0.00	62.200	0.972	
13				
0.00	0.0000	0.1500	0.2495	0.5140
10.00	0.4700	0.1329	0.2495	0.5140
20.00	0.9400	0.1815	0.2495	0.5140
25.00	1.1400	0.2335	0.2495	0.5140
30.00	1.2600	0.2763	0.2495	0.5140
35.00	1.3000	0.3016	0.2495	0.5140
45.00	1.2800	0.3373	0.2639	0.4820
60.00	1.2000	0.3938	0.2670	0.4820
75.00	1.0500	0.4866	0.2670	0.4820
90.00	0.8800	0.5811	0.2670	0.4820
120.00	0.4750	0.7282	0.2670	0.4820
135.00	0.2400	0.7598	0.2670	0.4820
150.00	0.0000	0.6800	0.2670	0.4820
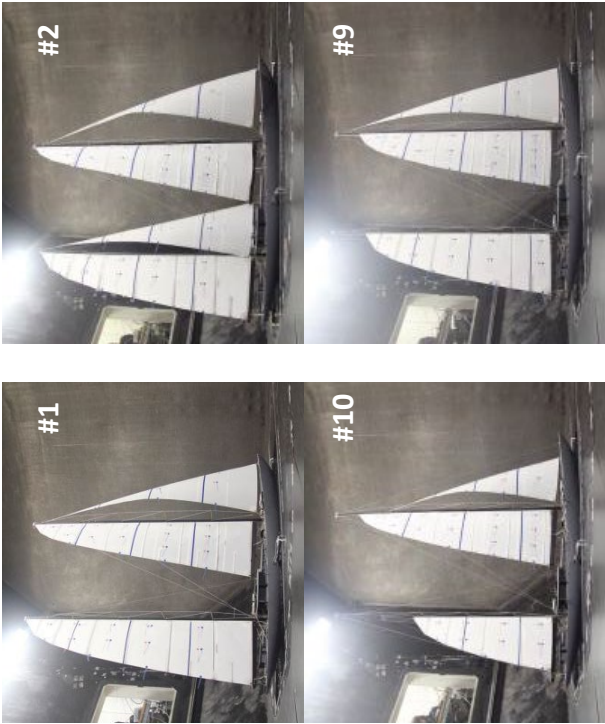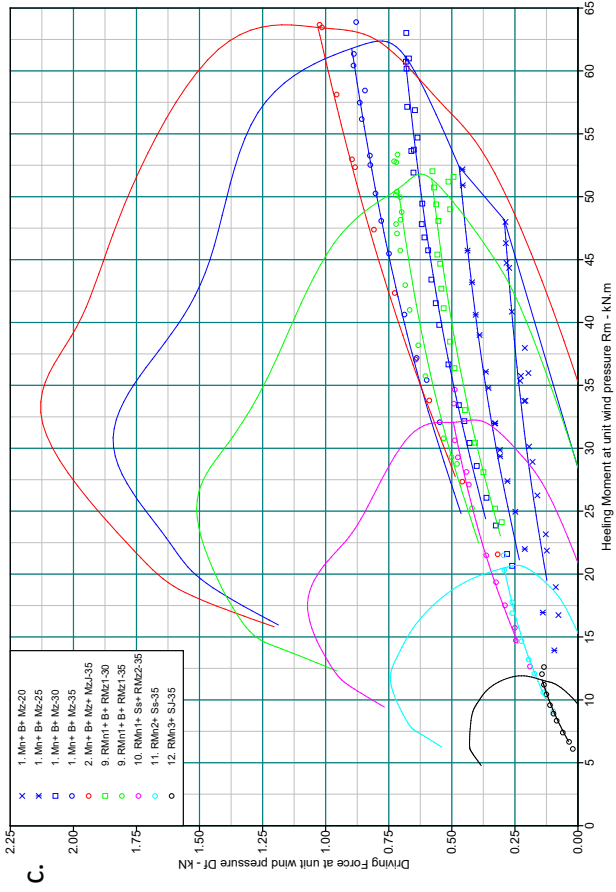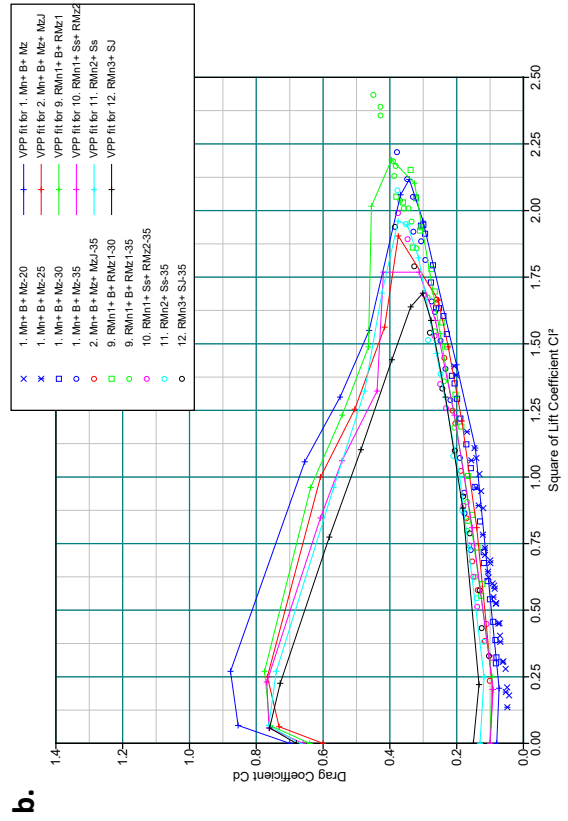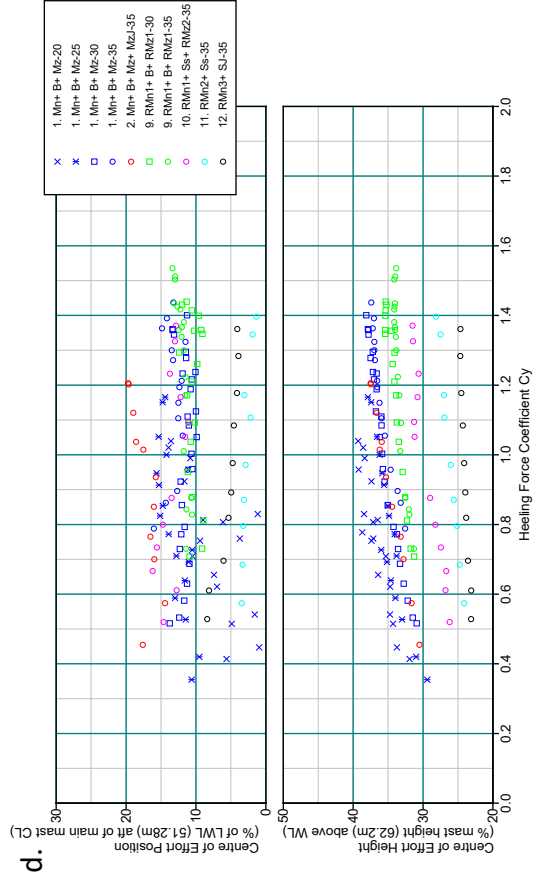
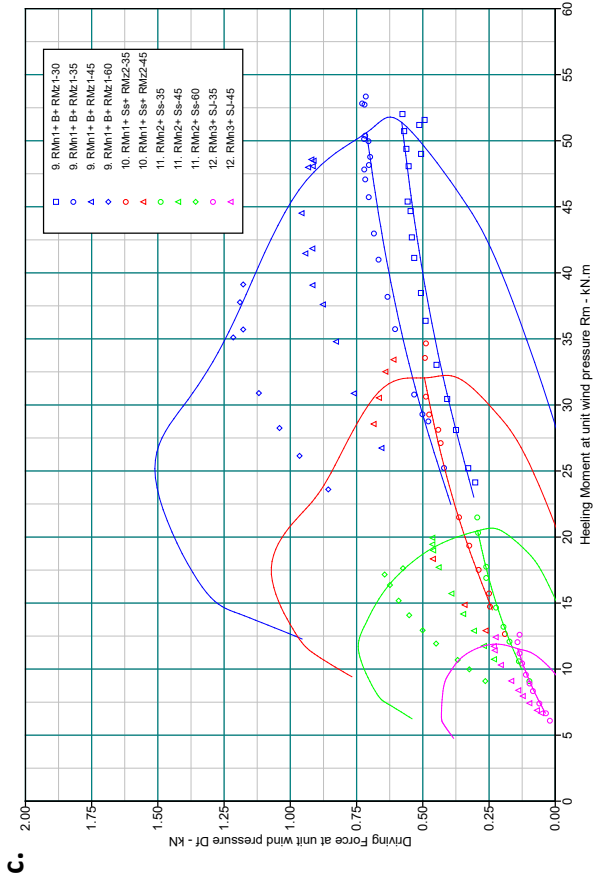**Figure A1. Test Results – Upwind.**
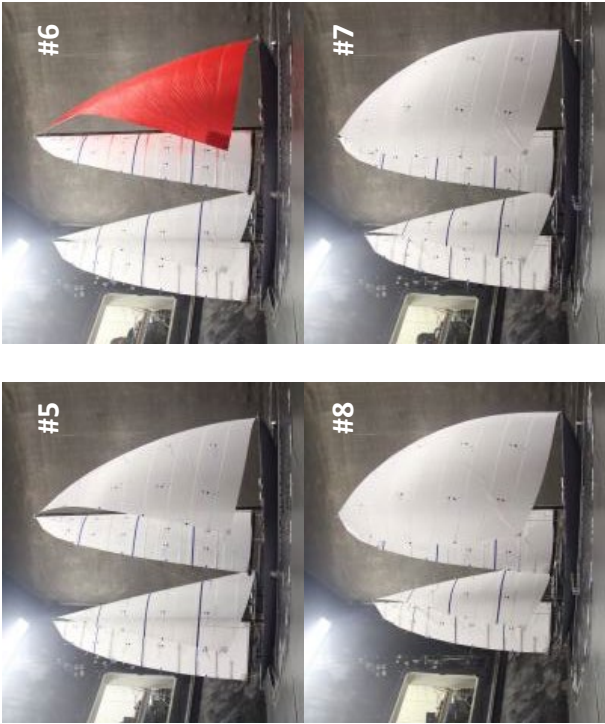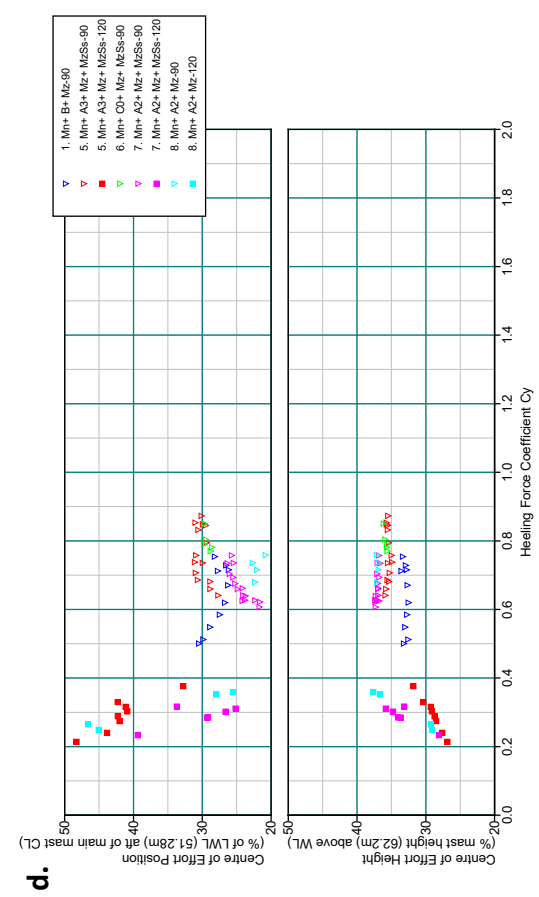
Figure A2. Test Results – Downwind.
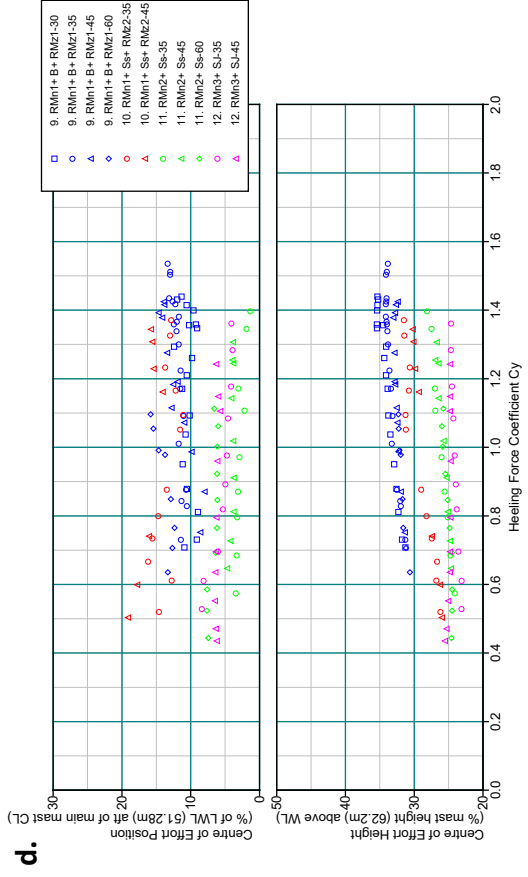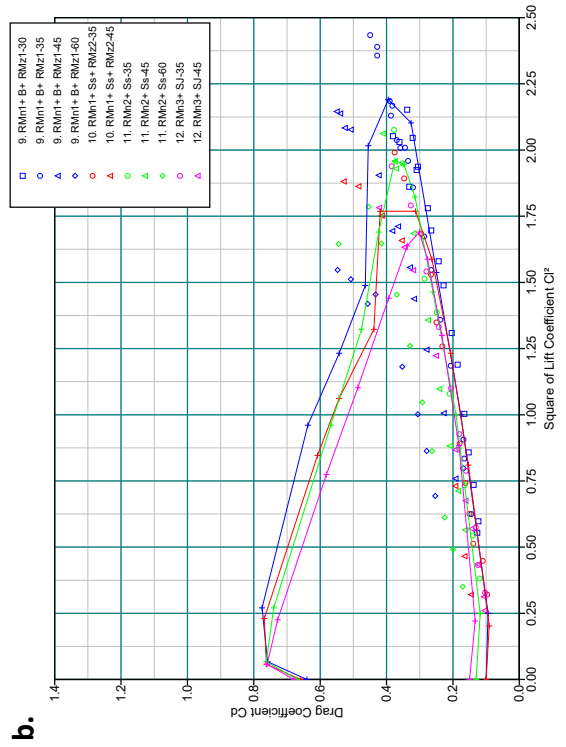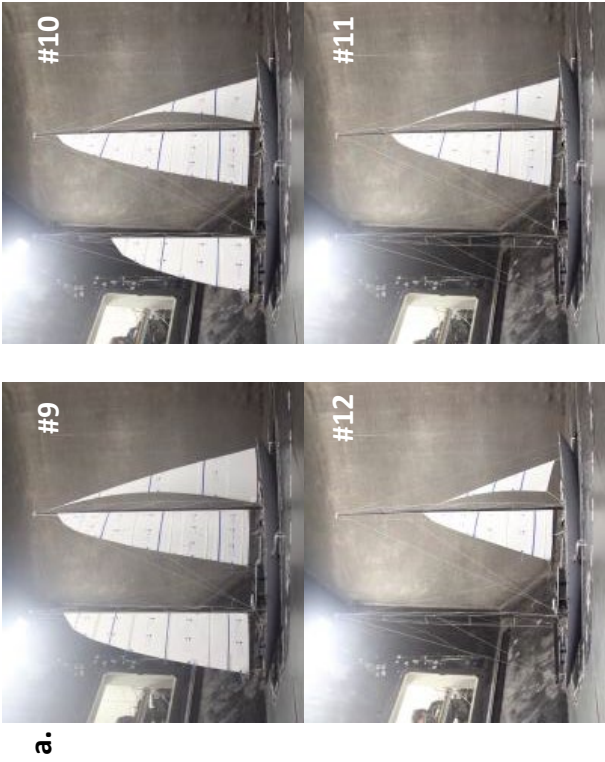
Figure A3. Test Results – Reefed Configurations.
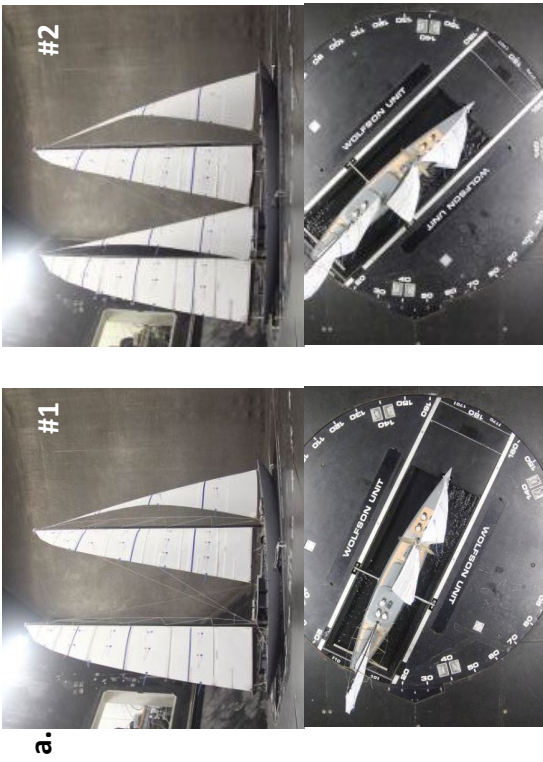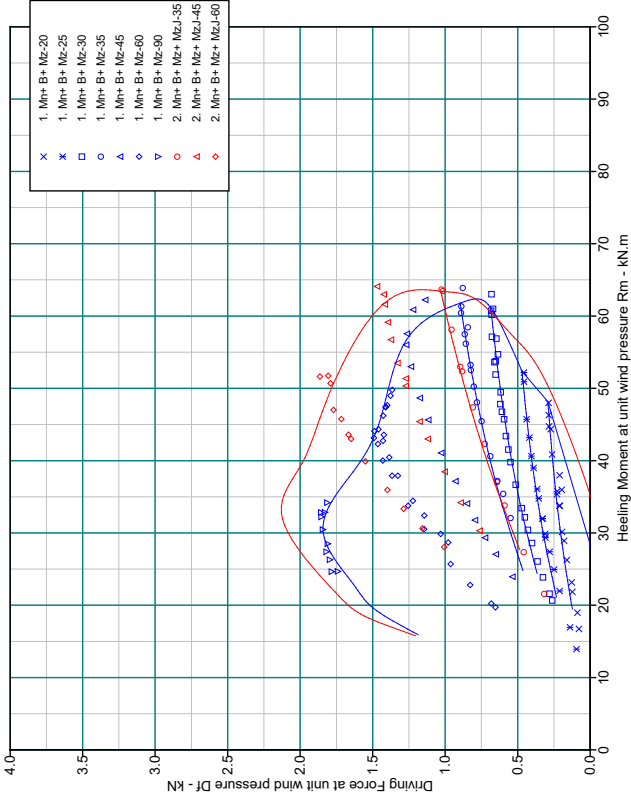
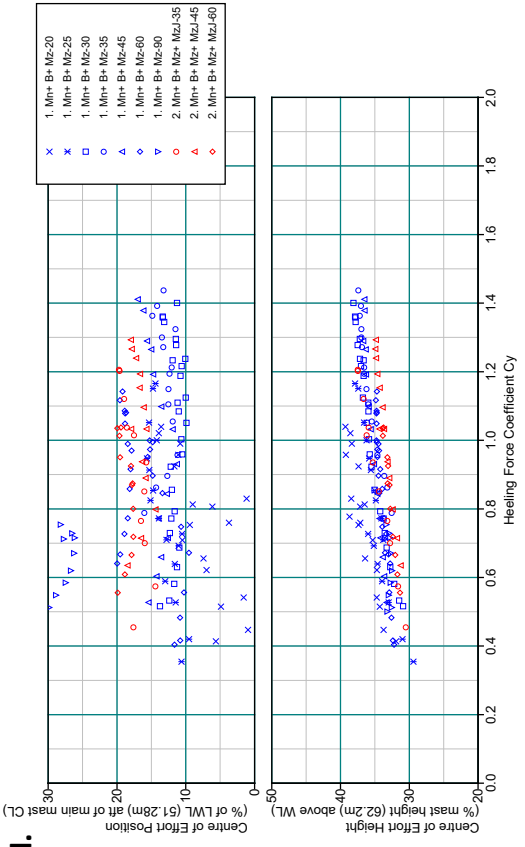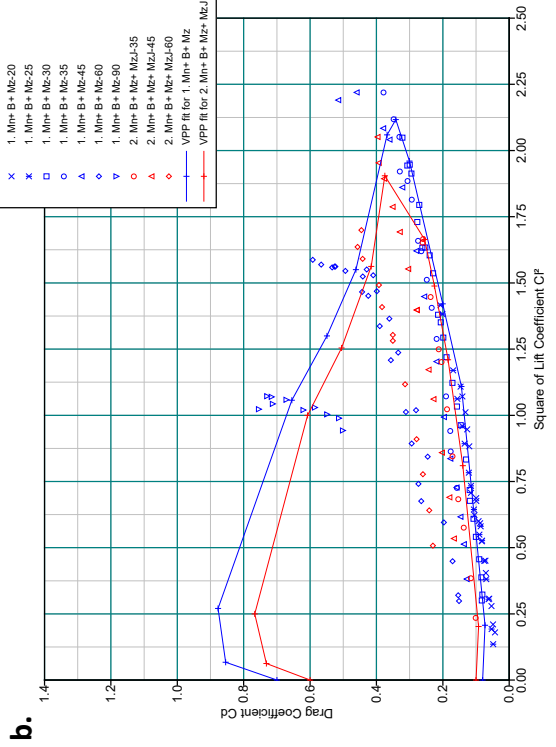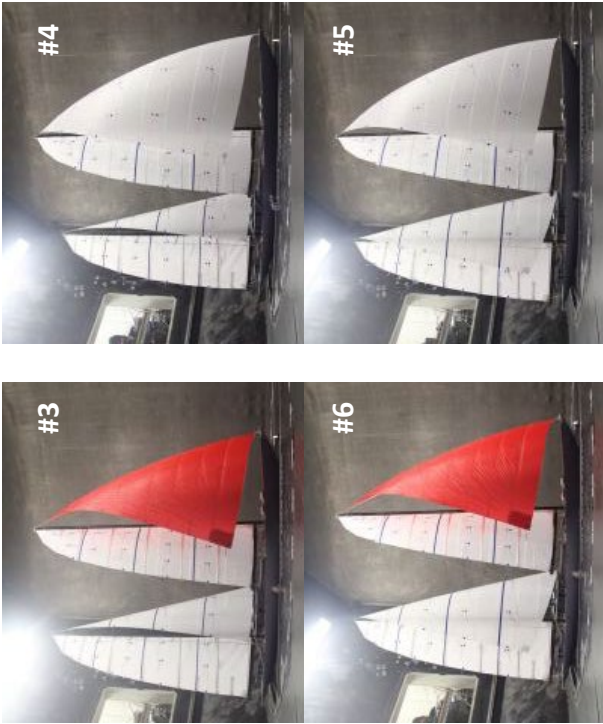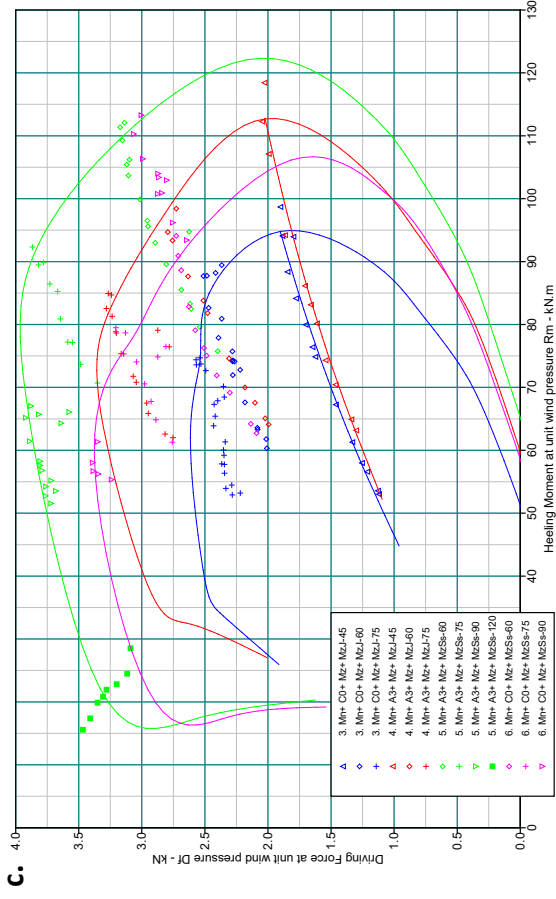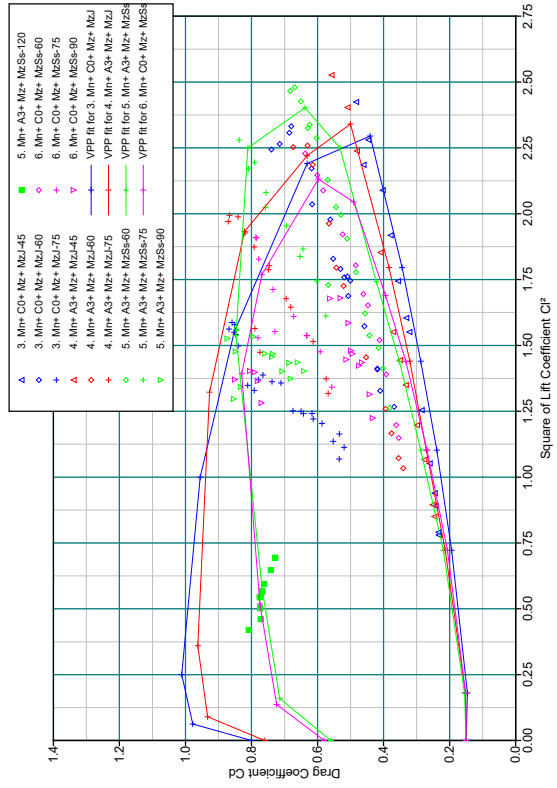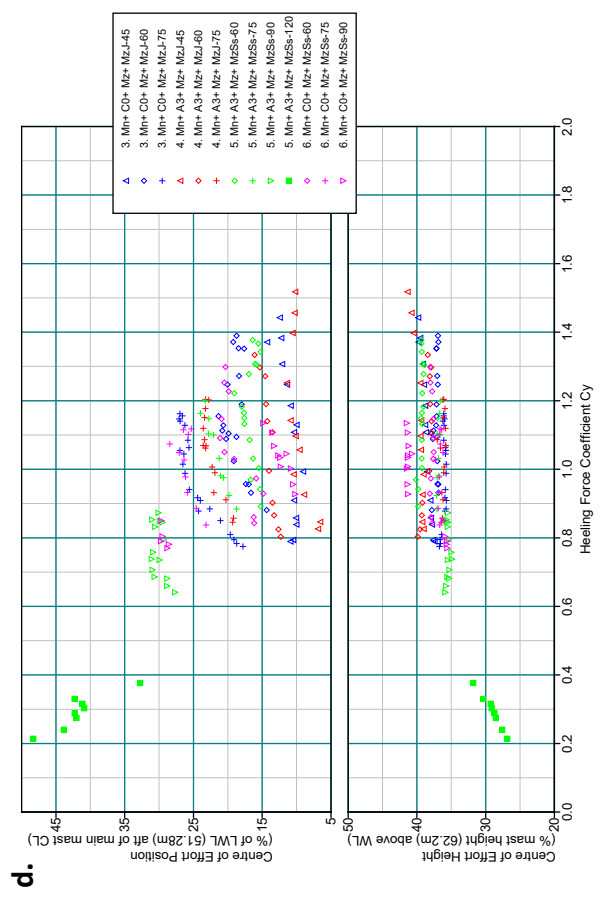**Figure A4. Test Results – Blade & Mizzen Jib Use.**

Figure A5. Test Results – Code 0 & A3 Use.